5.1. Introduction

Supramolecular chemistry is still a young field and related scientists are keenly involved in developing a variety of applications for the benefit of mankind[1][2]. Gels are supramolecular smart materials having a solid-like appearance that does not flow being predominantly liquid in composition and seem jelly-like materials[3][4]. Gels are commonplace in nature as well as occupy a prominent position in our lifestyle[5][6]. Increasingly, smart materials are being explored for their applications in multidisciplinary fields, including conductance[7], optical[8], sensing[9][10], drug delivery[2], and tissue engineering[11][12], catalytic[13], etc. Hydrogel is an important class of smart materials[14]. In the last decade, hydrogels were primarily synthesized through traditional molecules including fatty acids, lipids, and sugars, etc[15][16]. But, in the last few years, low molecular weight gelators (LMWGs) snatched the attention in gel synthesis due to their easy synthetic procedures and tunability in gel properties[17]. Organo hydrogels are comparatively more explored than metallohydrogels. The basic difference of organo hydrogel and metallohydrogel is the absence and presence of metal respectively[18]]. Further, inclusion of metal to organohydrogels may enhance the conductance, magnetic, color, catalytic[20], rheological properties[19]. Thus, these additional properties of exploration a viscoelastic gel like matrix which contains at least one metallic element is class of metallogel[21]. Taking into account, we headed our research towards synthesis of a conductive metallohydrogel which could be helpful in exploring the new dimensions of metallogel as a highly conductive material. In near future, these conductive metallogels may be used as electrolyte material in Li or Na ion batteries and may create a stable system for charge transport in various electrolytic cells[22]. In order to achieve our true target, we have designed a symmetrical chiral LMWG with suitably placed metal binding sites and directional H-

bonding. Because of the extensive applications of metallohydrogels in electrical[23], electronic[24], and optical devices[25], several researchers are highly concerned about the electrical characteristics and device-fabrication of these materials[4][26]. Our research division has been engaged in the manufacture of metal-semiconducting (M-S) junction type devices using metallohyrdogel. In addition, we want to figure out the manner in which the metallohydrogel utilizes its various functions. M-S based Schottky barrier formation is still a field of intensive research. A barrier forms at the interface between a metal and a semiconductor when it comes into contact with one[27].

In the present article, we report the fabrication of a supramolecular Mg(II)-allylamine (Mg-ALA) metallohydrogel using allylamine as the low molecular weight gelator (LMWG). Our study reveals that synthesized metallogel (Mg-ALA) is semiconducting and has been used to fabricate a thin-film device (Ag/Mg-ALA) at room temperature.The *I-V* characteristics of the Ag/Mg-ALA based thin-film device display a nonlinear rectifying behaviour, suggesting the formation of a Schottky Barrier diode[28][29].

5.2 Experimental

5.2.1. Material

Allylamine, magnesium nitrate hexahydrate, were acquired from S.D. Fine Private Ltd. Throughout the whole experiments, the chemicals were used without additional purification. Double-distilled water was used during experiments.

5.2.2. Characterization

The UV-vis spectra were conducted on a Thermo Scientific EVOLUTION 201 spectrophotometer. PerkinElmer Spectrum spectrophotometer was used for FT-IR

characterization. Rheology of metallogel was achieved on MCR 702 Twin Drive Rheometer. The SEM images were collected on EVO-Scanning Electron Microscope MA15/18. Powder

5.2.3. Synthesis of Mg(II)-based metallohydrogel (Mg-ALA)

The Mg(II)-metallohydrogel (Mg-ALA) was synthesized by the instantaneous mixing of 1 mLof an aqueoussolution of magnesium nitrate hexahydrate (0.291 g, 1 mM) and 500 µl of the allylamine ligand at room temperature instantaneously. The sustainability of the gel material was scrutinized by conventional inverted vial method. The minimum critical gel concentration (MGC) of Mg-ALA was determined through the variation of the concentration in the range of 100–300 mg/mL magnesium nitrate hexahydrate in aqueous medium and range of 100 to 500 µl of allylamine. MGC of Mg-ALA was found to be 300 mg/mL aqueoussolution of magnesium nitrate hexahydrate and 500 µl of allylamine.

5.2.4. Device fabrication

For metal-semiconductor (MS) junction device fabrication, an Indium doped Tin oxide (ITO) coated glass substrates (15×15 mm^2) are ultrasonically cleaned using standard wet cleaning subsequently in the soap solution for 20 minutes, deionized (DI) water for 15 minutes, acetone 10 minutes, and isopropanol for 10 minutes and finally treated by plasma cleaning in the presence of argon for 20 minutes. Initially, supramolecular Mg-based metallogel was deposited on the ITO coated glass substrate and annealed at 100^0C for 30 min. In the second step, ~80 nm thickness of metal (Ag) was deposited for a contact electrode by using a thermal evaporator unit. The evaporated metal (Ag) forms the circular dots of a 1 mm radius on the top of the semiconductor device using a shadow mask technique. The thicknesses of the Mg-ALA gel layer (~200 nm) were measured using the F20 Filmmetrics, USA instrument.[30]

5.3. Result and discussion

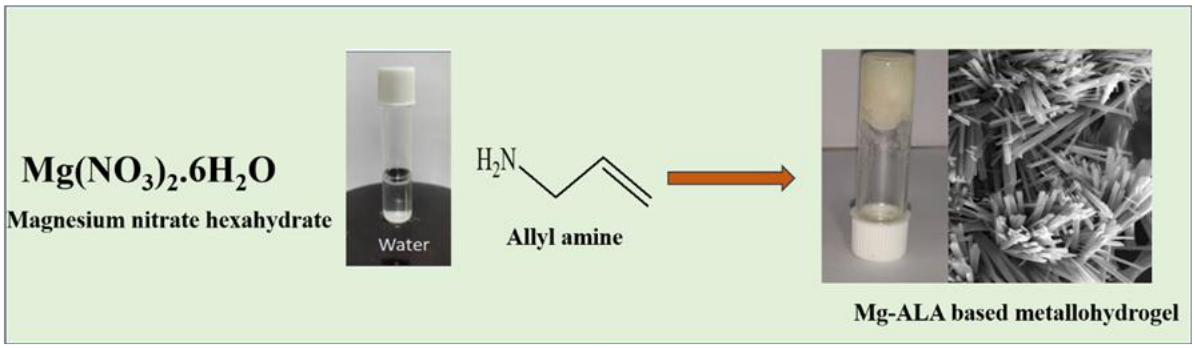

Scheme 5.1 Synthetic scheme of Mg-ALA based metallohydrogel

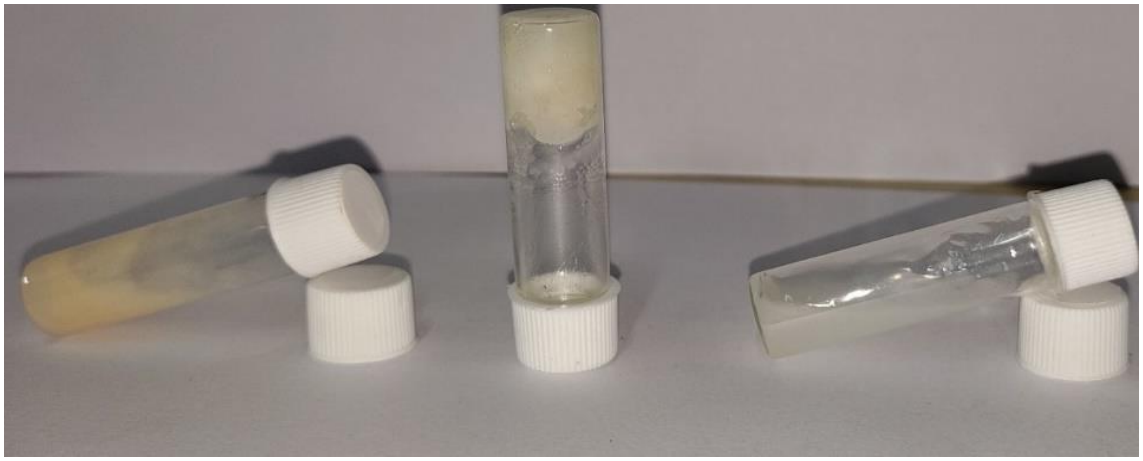

Figure.5.1 MGC of Mg-ALA was found to be 300 mg/mL aqueoussolution of magnesium nitrate hexahydrate and 500 µl of allylamine

The direct gelation test was performed by adding different metal cations such as Cd^{2+}, Co^{2+}, Zn^{2+}, Cu^{2+}, Ni^{2+}, Pb^{2+}, Mn^{2+}, Fe^{2+}, and Sn^{2+} into allylamine as LMWG gelator (ALA) in water, It can be noticeable that among these metal cations, specifically $Mg(NO_3)_2.6H_2O$ was capable to form a gel with gelator allylamine(ALA). The morphological characteristics of the synthesized metallogel was investigated by FESEM analysis.

5.3.1. Morphological study

The morphology of the Mg-ALA gel was studied using FESEM analysis. The resulting image **(Figure5.2**) reveals the structural characteristics of the material. The morphological pattern of the Mg-ALA gel is described as "agglomerated," indicating that the gel is formed by the aggregation of individual components into larger clusters. This agglomeration is likely due to the structural compactness of the material, suggesting that the components are closely packed together. The elemental analysis, which is likely represented in **Figure5.1.(c)-(f)** demonstrates the presence of several elements: C (carbon), N (nitrogen), O (oxygen), and Mg (magnesium). The presence of these elements confirms the composition of the Mg-ALA gel and indicates that the gel contains various chemical components.

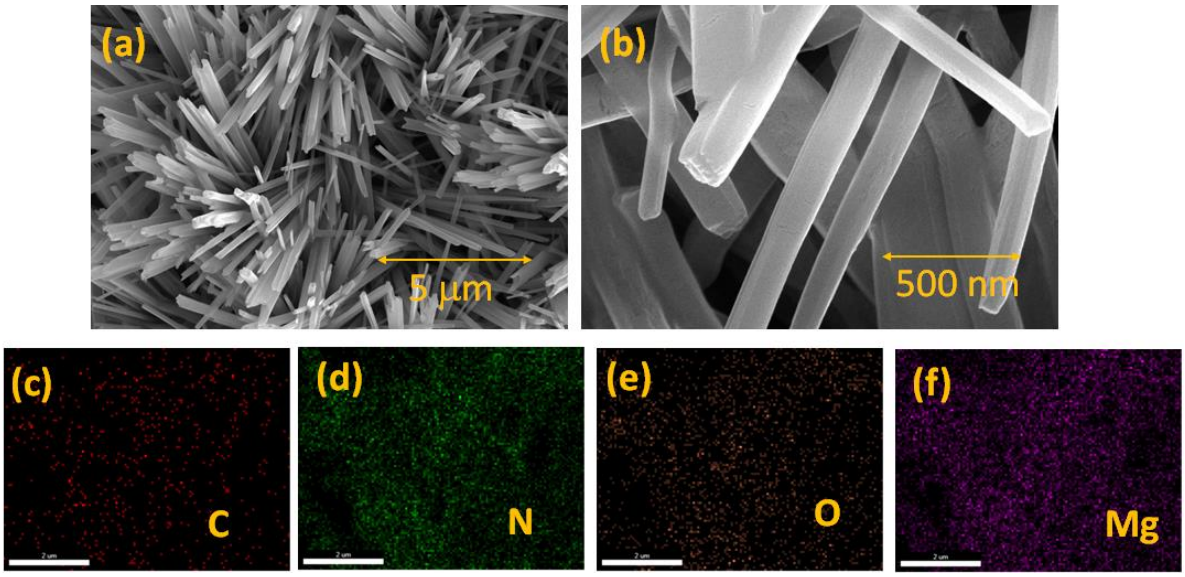

Figure.5.2 (a),(b) the SEM picture of vacuum-dried metallogel, and (c-f) elemental mapping of Mg-ALA hydrometallogel showing the presence of C, N, O, Mg elements.

The Mg-ALA metallogel was created through the action of ALA. This indicates that ALA was involved in the gelation process and played a role in forming the structural network of the gel. Several supramolecular facets such as hydrogen bonds, metal-LMWG connectivities, electrostatic interactions, hydrophobic interactions, and van der Waals forces between the Mg (II)-source and the metal-coordinating allylamine (LMWG) in water medium might be effective for self-assembly to occur to obtain the Mg (II) ion based stable supramolecular metallohydrogel.

5.3.2. UV-vis and FT-IR study

The behaviour of the ALA gelator with magnesium nitrate hexahydrate in water was observed by an analysis using UV-vis absorption spectroscopy. We passed out a titration experiment between the gelator (ALA) and Mg(II) metal ion **Figure5.3(a).** A colourless clear solution of gelator (ALA) ($1x10^{-4}$ M, DMF, 25^{o}C) existing a broadband 285 nm and 294 nm consistent to n-π* transition [34][35]. These alternate band appeared due to unlike planarity of ligand[31], after multiple additions of $Mg(NO_3)_2.6H_2O$ ($1x10^{-4}$M, water 25^{o}C), the band at 285 nm and 294 nm vanished enlightening that the Mg^{+2} had formed a complex with the gelator.

The FT-IR spectra of gelator and synthesized metallohydrogel shown in **Figure5.3(b).** The gelator ALA showed strong broad band in the region of 3030 cm^{-1} which arises due to the vibration of N–H groups. The FT-IR spectra of the gelator also showed vibration at 1370 cm^{-1} due to the (–NH), the xerogel has poor broadband in the region of 3436 cm^{-1} which suggests the -OH band of lattice/co-ordinated water molecules. The synthesized hydrogel did not show any band in the region of 3030 cm^{-1} (N-H); that attributed to loos of H atom in the complex. Thus, it could be expected that co-ordination of Mg^{+2} with the gelator (ALA).

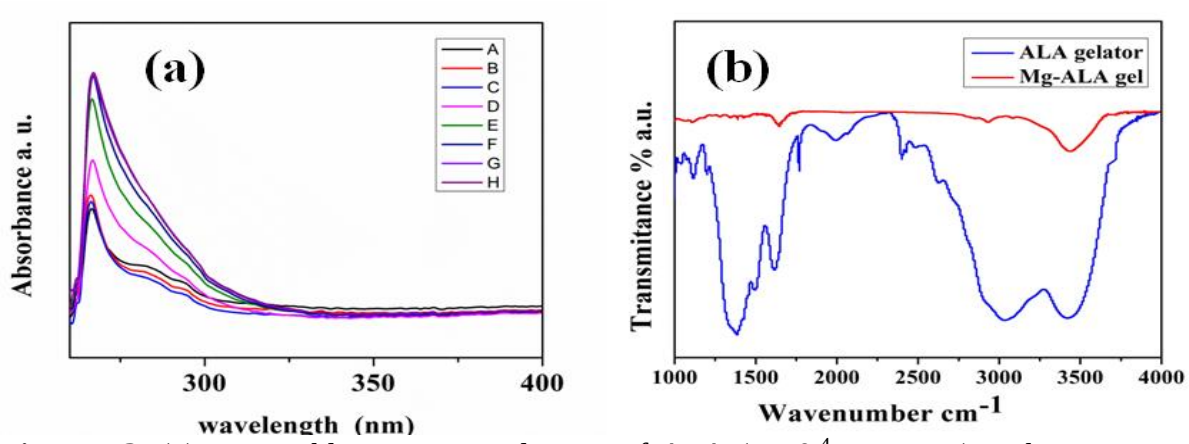

Figure.5.3. (a) UV-visible titration evaluation of ALA ($1x10^{-4}$ M, water) with magnesium nitrate hexahydrate in water ($1x10^{-4}$ M, water) and (b) FT-IR analysis of Mg-ALA hydrogel along with gelator ALA

5.3.3. Study of optical band gap of metallohydrogel

UV-Vis absorption study. The optical behavior of the Mg-ALA metallohydrogel was studied by UV-VIS absorption. **Figure5.3** shows the UV-Vis absorption spectra of the material. The absorption spectra were recorded in the wavelength range of 250–600 nm by a UV-VIS spectrophotometer and the energy absorption was found in the visible region. From the UV-VIS absorption spectra, the optical bandgap of our synthesized material can be calculated using the following standard Tauc's equation.

$$(\alpha h\nu)^2 = A(h\nu - Eg)$$

where Eg, h, α and ν stand for optical bandgap, Planck's constant, absorption coefficient, and frequency of light, respectively. 'A' which is unity in an ideal case, is a constant. With the extrapolation of the linear region of the plot $(\alpha h\nu)^2$ vs. hν **(Figure 5.4)** to α = 0 absorptions, the direct optical band gap (Eg) was evaluated as 4.1 eV for Mg-ALA metallohydrogel

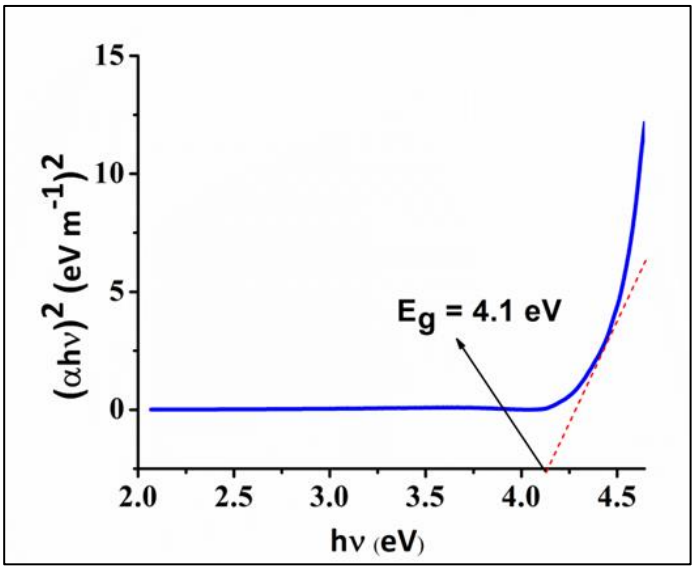

Figure.5.4. Bandgap measurement by Tauc's plot for Mg-ALA hydrometallogel

5.3.4. Rheological analysis

Rheology focuses on understanding how materials respond to applied forces and deformations. This can include how fluids flow (liquid-like behavior) or how solids deform under stress. Rheology often deals with complex materials that exhibit both solid and liquid properties. Viscoelastic materials have a combination of viscous (liquid-like) behavior, where they flow when subjected to force, and elastic (solid-like) behavior, where they return to their original shape when the force is removed.

The material being studied, the Mg-ALA based metallohydrogel, exhibits characteristics of both a solid and a liquid, which was confirmed by rheological analysis. The key parameters measured in rheology is Storage Modulus (G') and Loss Modulus (G"). Storage Modulus (G') represents the material's ability to store and recover elastic energy, while Loss Modulus (G") represents its ability to dissipate energy. At 25°C and a frequency of 10 rad.s^{-1}, G' was found

to be higher than G". This suggests that the material has more solid-like properties under these conditions. We have also observed that the value of intersection of G' and G" at a shear stress of ~1.7 Pa is significant. This point represents the gel-sol transition point, where the material shifts from a gel-like state to a more liquid-like state. It's essentially the point at which the gel structure starts breaking down. The frequency sweep experiment involved varying the applied frequency from 0.1 to 100 rad.s^{-1}. The observation that both G' and G" values increased linearly with increasing frequency suggests that the material retains its elastic nature over this frequency range. The result, where G' is consistently higher than G", indicates that the structural integrity of the Mg-ALA metallohydrogel is maintained over the range of conditions tested. This means that even as the material experiences stress and varying frequencies, it remains more solid-like in its behaviour.

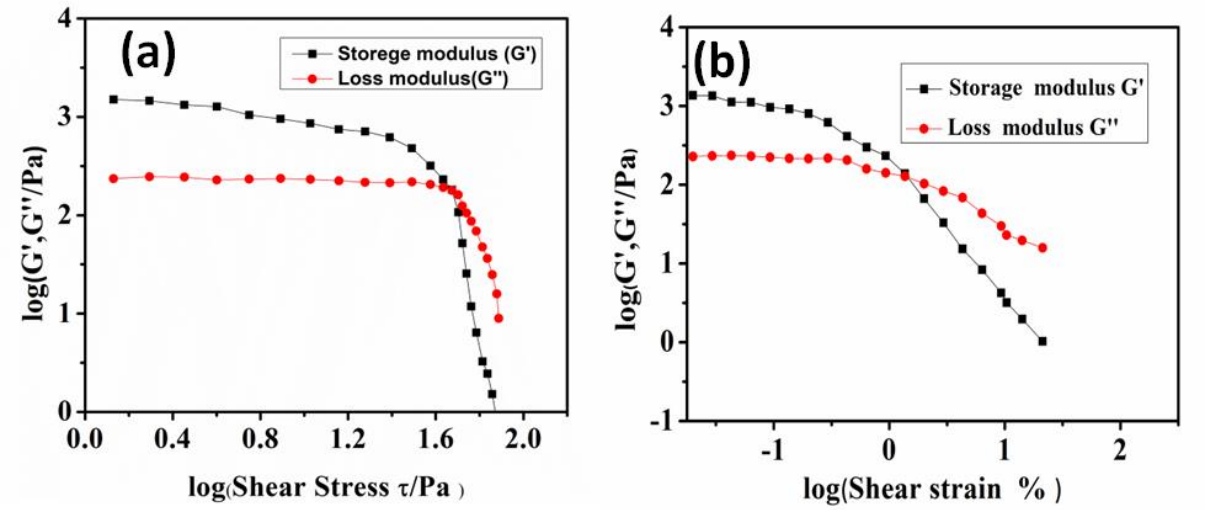

Figure.5.5. (a) Dynamic shear stress against G" and G′, (b) dynamic oscillation Strain vs G" and G′ for as synthesis metallohydrogel.

5.3.4. Strategy of device fabrication

A Schottky barrier diode was designed with the help of aforementioned optical properties of as-synthesised metallogel in **Figure5.6**

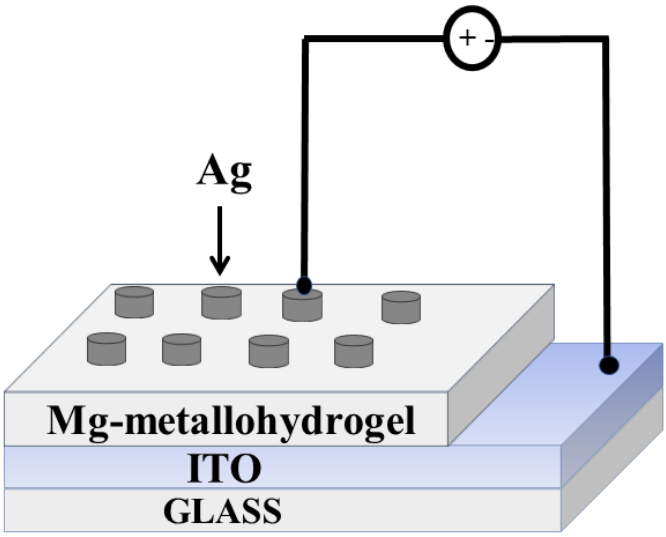

Figure.5.6 graphic fabricated device structure of Mg-ALA metallohydrogel based schottky barrier diode.

The Tauc's plot analysis in **Figure 5.4** demonstrates that the Mg-ALA metallohydrogel synthesized in its as-synthesized state falls within the category of semiconducting materials [43], [44]. Consequently, we have created a schottky barrier diode based on a junction between a metal (Ag) and a semiconductor Mg-ALA metallohydrogel (MS). This thin-film device was then subjected to current-voltage (I-V) measurements. The I-V measurements of the thin-film device, composed of an organo-metallogel Mg-ALA metallohydrogel, were conducted at room temperature using a Semiconductor parameter analyser (B1500A from Keysight, USA). The bias voltage ranged from -1.5V to +1.5V. The current was observed to be - A with a reverse bias of 2V and A with a forward bias of 1.5V. The rectification ratio (Ion/Ioff) of the Cu-TMA

based SBD at 1.5V was, indicating its superiority as a recently developed device. Furthermore, the I-V characteristics of the Ag/Mg-ALA metallohydrogel-based thin-film device **(Figure5.7)** were examined. The results revealed a non-linear rectifying behavior at the interface between Ag/Mg-ALA metallohydrogel, suggesting the formation of a schottky barrier diode.

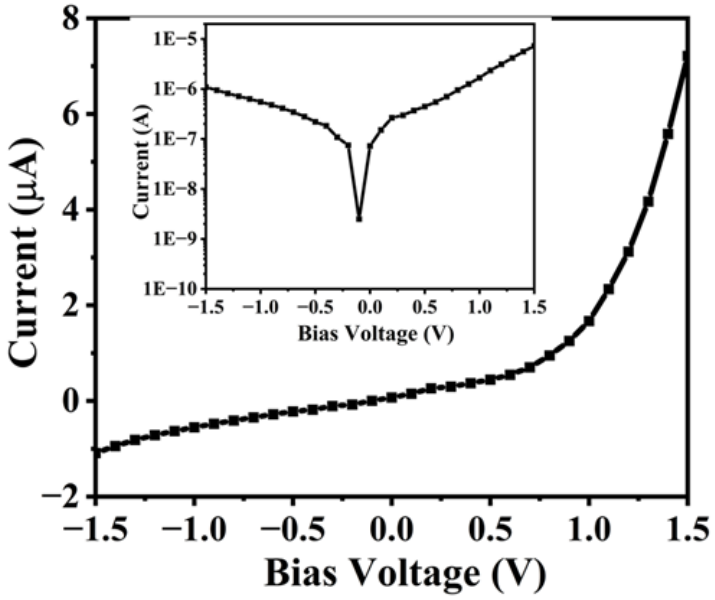

Figure.5.7 *I–V* characteristics graph for ITO/Cu-TMA/Ag-structured thin-film device.

5.4 Conclusion

We synthesized a stable supramolecular Mg-ALA metallohydrogel by combining magnesium nitrate hexahydrate and Allylamine (ALA) in a water-based solution. Rheological studies verified that these Mg-ALA metallogels possess a high storage modulus and remain thermally stable. The morphology and structure of the resulting supramolecular metallogel were characterized using UV-Vis, FT-IR (Fourier-transform infrared spectroscopy), and FESEM (Field Emission Scanning Electron Microscopy). To evaluate its semiconducting properties, we determined the energy band gap and explored various electrical behaviors, including

current-voltage characteristics and rectification in the metal-semiconductor (MS) junction-device. Additionally, exploiting the device's non-linear rectifying behavior, we successfully crafted an active electronic component a Schottky Diode. In conclusion, our developed semiconducting Mg-ALA metallogel exhibits great promise and efficiency, paving the way for potential applications in a wide range of future optoelectronic devices.

5.5 References

[1] J. K. Wychowaniec, H. Saini, B. Scheibe, D. P. Dubal, A. Schneemann, K. Jayaramulu, *Chem. Soc. Rev.* **2022**, *51*, 9068–9126.

[2] K. Sarkar, P. Dastidar, *Chem. - An Asian J.* **2019**, *14*, 194–204.

[3] M. K. Dixit, M. Dubey, *Phys. Chem. Chem. Phys.* **2018**, *20*, 23762–23772.

[4] S. Dhibar, A. Dey, A. Dey, S. Majumdar, D. Ghosh, P. P. Ray, B. Dey, *ACS Appl. Electron. Mater.* **2019**, *1*, 1899–1908.

[5] A. Meftahi, P. Samyn, S. A. Geravand, R. Khajavi, S. Alibkhshi, M. Bechelany, A. Barhoum, *Carbohydr. Polym.* **2022**, *278*, 118956.

[6] P. C. Marr, A. C. Marr, *Green Chem.* **2015**, *18*, 105–128.

[7] K. Hong, Y. K. Kwon, J. Ryu, J. Y. Lee, S. H. Kim, K. H. Lee, *Sci. Rep.* **2016**, *6*, 1–8.

[8] S. Diring, F. Camerel, B. Donnio, T. Dintzer, S. Toffanin, R. Capelli, M. Muccini, R. Ziessel, *J. Am. Chem. Soc.* **2009**, *131*, 18177–18185.

[9] O. Bunkoed, F. Davis, P. Kanatharana, P. Thavarungkul, S. P. J. Higson, *Anal. Chim. Acta* **2010**, *659*, 251–257.

[10] A. Sebastian, E. Prasad, *Langmuir* **2020**, *36*, 10537–10547.

[11] H. Li, J. Zhang, H. Xue, L. Li, X. Liu, L. Yang, Z. Gu, Y. Cheng, Y. Li, Q. Huang, *Mater. Horizons* **2023**, *10*, 1789–1794.

[12] N. Malviya, C. Sonkar, R. Ganguly, D. Bhattacherjee, K. P. Bhabak, S. Mukhopadhyay, *ACS Appl. Mater. Interfaces* **2019**, *11*, 47606–47618.

[13] S. Sarkar, S. Dutta, P. Bairi, T. Pal, *Langmuir* **2014**, *30*, 7833–7841.

[14] T. R. M., P. CHVS, Y. M., P. C. H., *Int. J. Curr. Pharm. Res.* **2021**, *13*, 12–17.

[15] Y. L. Wu, X. Chen, W. Wang, X. J. Loh, *Macromol. Chem. Phys.* **2016**, *217*, 175–188.

[16] C. A. Dreiss, *Curr. Opin. Colloid Interface Sci.* **2020**, *48*, 1–17.

[17] T. Feldner, M. Häring, S. Saha, J. Esquena, R. Banerjee, D. D. Díaz, *Chem. Mater.* **2016**, *28*, 3210–3217.

[18] Z. He, W. Yuan, *ACS Appl. Mater. Interfaces* **2021**, *13*, 1474–1485.

[19] S. Hao, C. Shao, L. Meng, C. Cui, F. Xu, J. Yang, *ACS Appl. Mater. Interfaces* **2020**, *12*, 56509–56521.

[20] A. Herrmann, R. Haag, U. Schedler, *Adv. Healthc. Mater.* **2021**, *10*, DOI 10.1002/adhm.202100062.

[21] M. K. Dixit, D. Chery, C. Mahendar, C. Bucher, M. Dubey, *Inorg. Chem. Front.* **2020**, *7*, 991–1002.

[22] M. Yu, J. Lin, Z. Wang, J. Fu, S. Wang, H. J. Zhang, Y. C. Han, *Chem. Mater.* **2002**, *14*, 2224–2231.

[23] W. Zhang, P. Feng, J. Chen, Z. Sun, B. Zhao, *Prog. Polym. Sci.* **2019**, *88*, 220–240.

[24] J. Lin, Q. Tang, J. Wu, S. Hao, *React. Funct. Polym.* **2007**, *67*, 275–281.

[25] Z. Xiong, P. Kunwar, P. Soman, *Adv. Opt. Mater.* **2021**, *9*, 1–11.

[26] A. Khan, M. Hussain, M. A. Abbasi, Z. H. Ibupoto, O. Nur, M. Willander, *Semicond. Sci. Technol.* **2013**, *28*, DOI 10.1088/0268-1242/28/12/125006.

[27] H. Sheng, S. Muthukumar, N. W. Emanetoglu, Y. Lu, *Appl. Phys. Lett.* **2002**, *80*, 2132–2134.

[28] Ö. Güllü, Ş. Aydoğan, A. Türüt, *Microelectron. Eng.* **2008**, *85*, 1647–1651.

[29] N. A. Al-Ahmadi, *Mater. Res. Express* **2020**, *7*, DOI 10.1088/2053-1591/ab7a60.

[30] R. K. Upadhyay, A. P. Singh, D. Upadhyay, A. Kumar, C. Kumar, S. Jit, *IEEE Electron Device Lett.* **2019**, *40*, 1961–1964.

[31] L. Wang, W. Qin, X. Tang, W. Dou, W. Liu, *J. Phys. Chem. A* **2011**, *115*, 1609–1616.